ELSEVIER

Journal of Pharmaceutical and Biomedical Analysis
19 (1999) 217–230

JOURNAL OF
PHARMACEUTICAL
AND BIOMEDICAL
ANALYSIS

Amperometric determination of xanthine and hypoxanthine at carbon electrodes. Effect of surface activity and the instrumental parameters on the sensitivity and the limit of detection

Éder T.G. Cavalheiro [a,b], Anna Brajter-Toth [a,*]

[a] *Department of Chemistry, University of Florida, Gainesville FL 32611-7200, USA*
[b] *Departamento de Química, Universidade Federal de São Carlos, CxP676, CEP 13565-905, São Carlos/SP, Brazil*

Received 22 January 1998; accepted 11 May 1998

Abstract

The performance of active graphite and carbon fiber surfaces produced by different mechanical/electrochemical methods of surface activation has been investigated in the amperometric determinations of xanthine and hypoxanthine under physiologically relevant conditions. The electrodes showed better limits of detection (LOD) when used with differential techniques with a capability of discriminating the analytical signal from the background. Square wave voltammetry and cyclic voltammetry showed the most sensitive response. Electrochemically activated carbon fiber ultramicroelectrodes showed the highest sensitivity (58 A M^{-1} cm^{-2}) and the LOD in the 200 nM range was observed at the rough pyrolytic graphite electrodes by square wave voltammetry. The results demonstrate the feasibility of the development of new electroanalytical methods for the determination of oxypurines in biological samples.

Keywords: Xanthine; Hypoxanthine; Amperometric determination; Graphite surface activation; Carbon fiber ultramicroelectrodes

1. Introduction

Oxypurines, hypoxanthine (HX), xanthine (XA) and uric acid (UA) are formed during purine metabolism and are found in tissues and body fluids such as blood and urine [1]. HX and XA are formed as a result of adenosine-5′-triphosphate (ATP) conversion to adenosine-5′-monophosphate (AMP), and then to HX and XA, via inosine-5′-monophosphate or adenosine pathways [2].

Determinations of extracellular concentrations of purines are of considerable significance because changes in the concentrations of purines can indicate several disfunctions or diseases. For example, excessive accumulation of uric acid (UA), produced as the final purine metabolite from HX and XA, can be a result of gout [1]. In heart perfusates

* Corresponding author. Tel.: +1 352 3927972; fax: +1 352 3924651; e-mail: atoth@pine.circa.ufl.edu

0731-7085/99/$ - see front matter
PII S0731-7085(98)00128-9

or dialysates elevated levels of purines can be an indicator of a heart attack since extracellular purines are also a marker of the level of cellular energy metabolism [3].

Many methods have been developed for the determination of XA and HX including stripping of Cu(II) complexes of purines [4–8], adsorptive stripping of purines from mercury [9], and direct determinations by linear sweep [10] and differential pulse voltammetry [11] at graphite, with limits of detection in the pM, submicromolar and micromolar range, respectively.

Enzyme and polymer modified electrodes [12–16] have also been investigated for selectivity and sensitivity in the determinations of XA and HX. Catalytic activity of the enzyme xanthine oxidase which selectively converts both purines in the presence of O_2 to UA and hydrogen peroxide has been exploited in these measurements. Direct electron transfer to the enzyme, electron transfer to the oxygen cofactor, and to the products of the enzymatic reaction hydrogen peroxide and uric acid are the methods that have been used to obtain the signal of XA and HX at the enzyme modified electrodes. Limits of detection in the micromolar range have been achieved by these methods.

In spite of these advances, determinations of purines at low concentrations under physiological conditions remain a challenge. Particularly challenging are the determinations under conditions when the purine signal is transient. In such determinations submicromolar sensitivity is often required in real time measurements in order to preserve the information content transmitted by the changing concentrations of purines.

We have shown previously that a strategy to optimize the determinations of purines requires fabrication of an active electrode and requires the development of an optimized method of acquisition of the purine signal in order to obtain a sensitive response [17,21]. An active electrode is expected to have a large active surface area with high density of surface sites for the interactions and for rapid electron transfer during the determination of purine concentration [17,21]. It has been shown previously that surface interactions which involve weak adsorption of the analyte at an active electrode, when rapid electron transfer is facile, contribute to a sensitive analyte response [17,18]. Finally, an electrode with a stable background current that can be subtracted or otherwise minimized is needed [17,21]. Active graphite electrodes that can be prepared by procedures combining electrochemical pretreatment and surface modification are a good candidate for these determinations [17].

The purpose of the work described here was to produce active electrodes by different methods of surface activation/pretreatment and to evaluate the sensitivity of the active electrodes in the determinations of purines XA and HX under physiologically relevant conditions. Different methods were compared for their sensitivity toward the purine signal and for their efficiency in discriminating the signal from the background current. Finally, the effect of efficient mass transport of the analyte on the response of purines at active electrodes was evaluated.

2. Experimental

2.1. Reagents

All chemicals were used as received. XA and HX were purchased from Sigma. Phosphate buffer was 70 mM. $K_3[Fe(CN)_6]$ (Fischer) and KCl (Fischer) were also used.

2.2. Apparatus

All measurements were performed with a BAS-100. The working electrode was a rough pyrolytic graphite (RPG) electrode (ca. 0.04 cm^2 area) that was prepared as described earlier [18]. The RPG was polished before each experiment on a 600-grit silicon carbide paper (Mark V Laboratory) on a polishing wheel (Ecomet I, Beuhler) followed by exhaustive rinsing with water. The auxiliary electrode was a Pt wire of ca. 0.17 cm^2 area and the reference electrode was the saturated calomel electrode (SCE). The RPG electrode area was determined by chronocoulometry with 5.0 mM $Fe(CN)_6^{3-}$ in 0.5 M KCl ($D_o = 7.36 \times 10^{-6}$ cm^2 s^{-1}) [19]. The potential window was from 0–1 V for purines and 0.4–0 V for ferricyanide.

The sensitivity in cyclic voltammetry (CV) was determined at 100 mV s^{-1}. Differential pulse voltammetry (DPV) parameters were 50 mV pulse amplitude, 50 ms pulse width, 17 ms sampling width, and 20 mV s^{-1} scan rate. Square wave voltammetry (SWV) was performed at 60 Hz with a step height of 2 mV, square wave amplitude of 20 mV (scan rate 120 mV s^{-1}). Frequency of 15 Hz/4 mV (60 mV s^{-1}) and 50 Hz/2 mV (100 mV s^{-1}) resulted in lower sensitivity. The solution pH was measured with a Corning 130 pH meter.

2.3. Ultramicroelectrode measurements

The BAS-100 with a home built pre-amplifier [20] was used in the measurements. The ultramicroelectrodes (UMEs) were constructed [21] by attaching a Cu wire (20 gauge) to a ca. 7 μm diameter carbon fiber (Textron Speciality Materials 744-44-0) with silver epoxy (EPO-TEC 410 E, Epoxy Technology); the epoxy was then cured at room temperature for 48 h. The carbon fiber was next sealed in a pipette tip with an epoxy resin (Resin 828, Shell) which was prepared by mixing the resin and hardener, *m*-phenylenediamine (MPDA) in 10:1.5 ratio (resin:hardener) in a 80°C water bath. The epoxy was cured for 24 h at room temperature and finally at 100°C for 1 h. The measurements were performed in a two electrode configuration with an SCE as the reference electrode.

The carbon fiber electrodes were polished on a 600-grit silicon carbide paper to remove the excess epoxy followed by a brief polishing with γ-alumina (0.1 μm particle size, Fischer) on an Alpha A polishing cloth (Mark V Laboratories) using a polishing wheel (Ecomet I, Beuhler). Finally the Cu wire was covered with a heat shrinkable tubing and a pin connector was soldered at the end. The electrodes were soaked in 2-propanol for 5 min and were next sonicated for 5 min in water.

In addition to the treatment described above carbon fiber UMEs were prepared by polishing on 150-grit silicon carbide paper first, followed by polishing on 600-grit paper and with γ-alumina, followed by final sonication in water for 5 min.

Carbon fiber electrodes were also prepared by an electrochemical pretreatment that has been optimized previously for the determination of oxypurines [21]. Briefly, the initially polished (600-girt/alumina) electrodes were continuously cycled (30 min) in the potential window between -1.0 and 1.5 V at 10 V s^{-1} in 70 mM phosphate buffer (pH 7.4). The electrodes were used shortly after treatment and were stored in phosphate buffer.

The potential window was 0.4–0.0 V for ferricyanide and 0.3–0.9 V for XA. The radius, *r*, of the carbon fiber UMEs was determined from the steady state current of $Fe(CN)_6^{3-}$ at 0.0 V in 0.5 M KCl ($D_o = 7.63 \times 10^{-6}$ cm^2 s^{-1}) [19] at different concentrations (1–10 mM) of $Fe(CN)_6^{3-}$. The CV scan rate was 100 mV s^{-1}. At carbon fiber UME XA current was measured at 0.700 V and the background was subtracted by extrapolation of the baseline obtained in the presence of the analyte in solution.

2.4. Procedure

XA and HX stock solutions were prepared in 70 mM pH 7.4 phosphate buffer before measurements. In CV determinations of the dependence of XA maximum current (i_p) and potential (E_p) on pH at the RPG electrode the concentration of XA was 100 μM. The pH was adjusted with NaOH and HNO_3. XA diffusion coefficients were obtained at a carbon fiber UME from the steady state current of 20 and 67 μM XA in 70 mM phosphate buffer pH 7.4.

At the RPG electrode the background current was measured and subtracted from the maximum current of the analyte by extrapolation of the baseline. The limit of detection (LOD) was determined as the concentration at which the maximum analyte current (i_p) was three times the background current at the potential (E_p) of the maximum current. This method was used to estimate the LOD rather than the method based on three standard deviations of the background current because of the non-random fluctuations of the background. At carbon fiber UMEs that have been polished XA current was measured at 0.700 V and the background was subtracted by extrap-

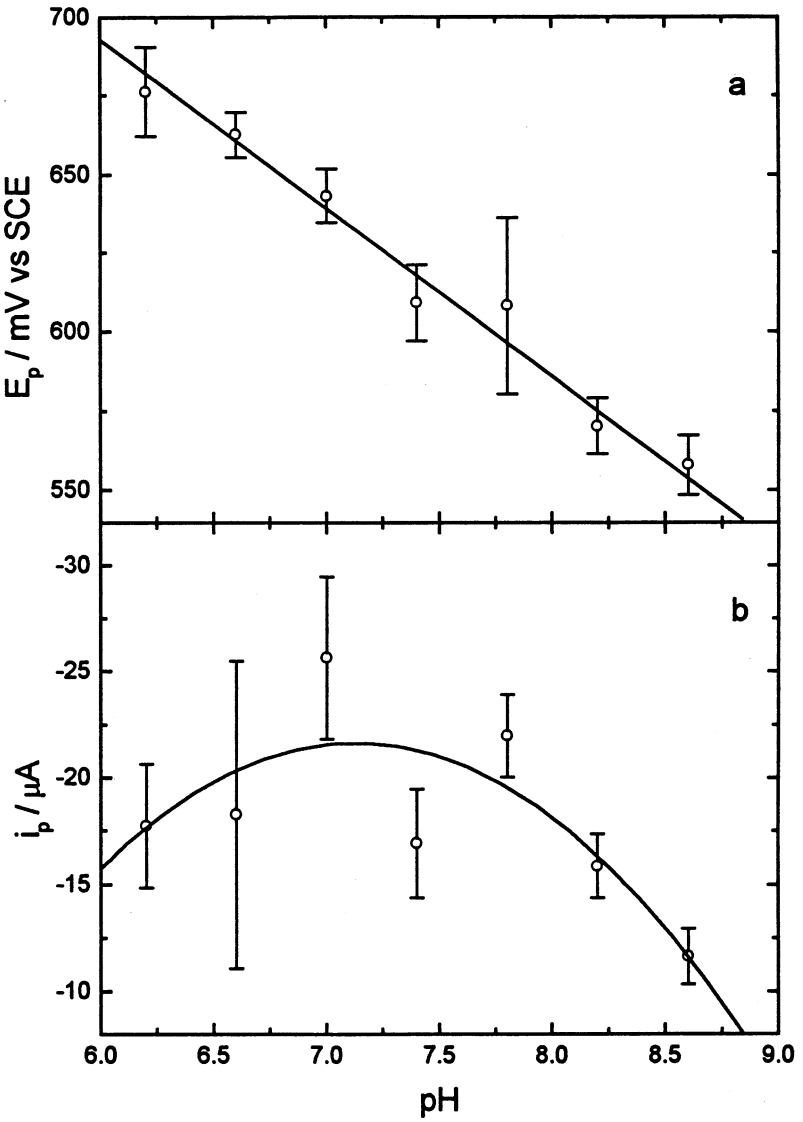

Fig. 1. Oxidation potential E_p (a) and current i_p (b) dependence on pH of 100 μM XA at the RPG electrode polished on 600-grit silicon carbide paper in cyclic voltammetry in 70 mM phosphate buffer (scan rate $v = 100$ mV s^{-1}, electrode area 0.04 cm^2).

olation of the baseline obtained in the presence of the analyte in solution. On the carbon fiber UMEs that have been electrochemically pretreated XA current was measured in the plateau region of the *i-E* curve in the 0.650–0.700 V range and the background was measured and subtracted by extrapolation of the baseline.

All measurements were performed at room temperature.

3. Results and discussion

3.1. Cyclic voltammetry of XA at the RPG electrodes

The effect of pH on the electrochemical oxidation of purines has been reported [10,11,22]. The oxidation of XA and HX is an overall 4e, $4H^+$ process at $pH < pK_{a1}$ (7.44; pK_{a2} 11.12 for XA

Table 1
Xanthine oxidation potential (E_p) dependence on pH at pyrolytic graphite electrodes

pH Range	E_p/V (versus SCE)	Ionic strength (mM)	Scan rate (mV s^{-1})	Reference
6.2–8.6[a,d,e]	1.01–0.054 pH	70	100	this work
3–8[b,d,e]	1.11–0.063 pH	500	200	[11]
0–12.5[b,c,e]	1.07–0.060 pH	500	3.3	[22]
2.9–7.7[a,c,f]	1.00–0.050 pH	500	20	[10]
7.7–10.6[a,c,f]	0.85–0.039 pH			

[a] Phosphate buffer.
[b] McIlvaine, ammonia or acetate buffer.
[c] Linear sweep voltammetry.
[d] CV.
[e] Rough surface.
[f] Mirror-like surface.

[23]) which proceeds in two 2e, $2H^+$ steps generating uric acid diimine and 6,8-dioxypurine as the oxidation products, respectively [22,24]. The first oxidation step in both reactions involves an addition of an oxygen to the C8 of the purine ring [22,24]. Fig. 1 shows the dependence of the oxidation peak potential E_p (Fig. 1a) and the peak current i_p (Fig. 1b) of XA on pH at the RPG electrode from CV. The results are summarized in Table 1 together with the results from previous work. The dependence of E_p on pH observed here supports the findings of Hansen and Dryhurst [22] who also used the RPG electrodes prepared by the procedure used here. Based on the results of this and previous work [22] in the oxidation of XA, the number of electrons and protons in the potential controlling process is constant with pH.

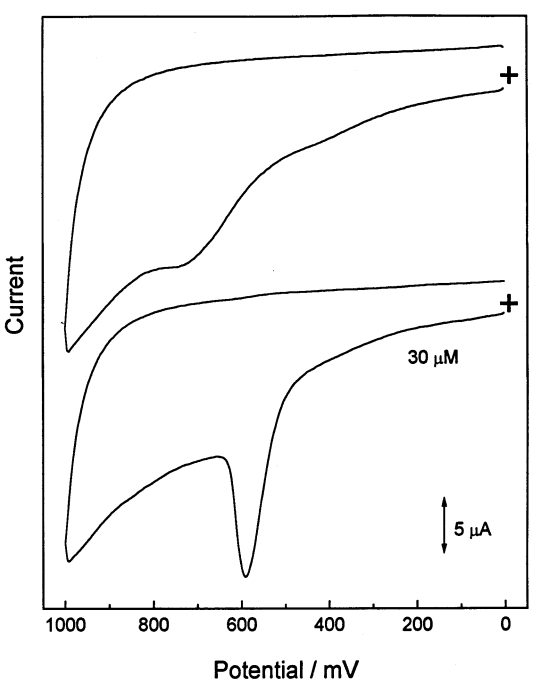

Fig. 2. Cyclic voltammograms of: XA (30 μM) in 70 mM phosphate buffer pH 7.4 (bottom curve) and buffer background (top curve) at the RPG electrode. Experimental conditions as in Fig. 1.

The dependence of E_p of XA on pH in Fig. 1a can be summarized by Eq. (1):

$$E_p = (1.01 \pm 0.02\ \text{V}) - (0.054 \pm 0.001\ \text{V/pH})\ \text{pH} \quad (1)$$

The 54 mV slope of the linear E_p versus pH plot (Eq. (1)) is below the theoretical Nernstian value of 59 mV [25]. The theoretical Nernstian slope of 59 mV is expected for a simple reversible reaction. The lower slope obtained here indicates a more complex process and is consistent with a contribution of adsorption to the electrochemical oxidation of XA at the RPG electrode. Surface interactions of XA at the RPG electrodes at pH 7.4 in 70 mM phosphate buffer were confirmed by CV where the log i_p versus log scan rate plots had a slope of 0.58 ± 0.04 and 0.70 ± 0.02 for 20 and 100 μM XA, respectively. The expected slope of this plot for a simple diffusion-controlled process is 0.5 and for an adsorption-controlled process is 1 [25]. The values obtained here which lie between

Table 2
Amperometric analytical figures of merit for xanthine (XA) and hypoxanthine (HX)[a]

Technique	Limit of detection[b] (μM)	Linear range (μM)	Sensitivity (A M^{-1} cm^{-2})	Sens $_{exp}$/ Sens $_{calc}$	r	Intercept
CV-RPG[c]	4	6–15	13.8 ± 0.25	25.8[e]	0.999	2.44 ± 0.10 μM
DPV-RPG[c]	0.8	0.8–30	5.2 ± 0.1	9.89[f]	0.996	-70 ± 8 nM
SWV-RPG[c]	0.2	2–10	12.2 ± 0.8	8.53[g]	0.995	0.36 ± 0.16 μM
CV-UME ECP[c]	6	6–15	57.8 ± 3.9	8.69[h]	0.998	-22 ± 4 pM
CV-UME 600 grit[c]	6	6–15	15.9 ± 0.3	2.39[h]	0.999	-9.3 ± 0.6 pM
CV-RPG[d]	4	6–50	4.8 ± 0.1	9.03[e]	0.999	0.74 ± 0.04 μM

[a] Phosphate buffer (70 mM) pH 7.4. RPG electrode resurfaced between measurements. UME (carbon fiber) treated as described in the text. Area: RPG 0.04 cm^2, UME 2.6×10^{-7} cm^2 (radius $= 2.8 \times 10^{-4}$ cm). Scan rate: CV 0.1 V s^{-1}, DPV 0.02 V s^{-1}, SWV 0.12 V s^{-1}. ECP, electrochemically pretreated; 600 grit—polished and alumina.
[b] Limit of detection, $S = 3\times$ background at potential of maximum current.
[c] XA.
[d] HX.
[e] Sens. calc. from [25]: $i_{irrev}(CV) = 2.99 \times 10^5\ n\ (\alpha n_a)^{1/2}$ A C $D^{1/2}\ v^{1/2}$, $\alpha n_a = 0.5$, $n = 4$ (XA, HX), $D = 4 \times 10^{-6}$ cm^2 s^{-1} (XA, HX).
[f] Sens. calc. from [31]: i_{irrev} (DPV) $= [n$ F A $D^{1/2}\ C\ \pi^{-1/2}\ t_p^{-1/2}]\ \Psi$, $t_p = 50$ ms, $\Psi = 0.27$, $\alpha = 0.5$, $n = 4$ (XA, HX), $D = 4 \times 10^{-6}$ cm^2 s^{-1} (XA, HX).
[g] Sens. calc. from [31]: i_{irrev} (SWV) $= [n$ F A $D^{1/2}\ C\ \pi^{-1/2}\ t_p^{-1/2}]\ \Psi$, $t_p = 8.4$ ms, $\Psi = 0.30$, $\alpha = 0.5$, $n = 4$ (XA, HX), $D = 4 \times 10^{-6}$ cm^2 s^{-1} (XA, HX).
[h] Sens. calc. from [34,35]: $i = 4\ n$ F D $r\ C$, $n = 4$, $D = 4 \times 10^{-6}$ cm^2 s^{-1} (XA).

the expected values indicate contributions from diffusion and adsorption to the electrochemical oxidation of XA [17].

As shown in Fig. 1b XA current (i_p) also depends on pH and shows a maximum around pH 7.2 near pK_{a1} of XA. The current decreases below and above the maximum pH which may reflect changes in the activity of the electrode surface and the analyte charge with pH. At higher pH the rate of oxidation of the graphite electrode surface is fast which can contribute to a loss of surface activity because of the formation of inert surface oxides [17,26].

A voltammogram of XA and of the background current at the RPG electrode (in pH 7.4 phosphate buffer) is shown in Fig. 2. The background current at the XA oxidation potentials around 0.550–0.600 V is not sufficiently stable to be used in direct background subtraction. The peak at 0.720 V observed in the background decreases in the presence of XA. The nature of this peak was not investigated further. The LOD of XA in CV estimated from the voltammograms is 4 μM (0.550 V at 100 mV s^{-1}, Table 2.

The non-linear behavior of the current (i_p) with the concentration of XA at the RPG electrode shown in Fig. 3 illustrates the effect of surface processes on the oxidation current. Surface interactions and enhanced rate of electron transfer become apparent as the concentration of XA decreases and can contribute to the non-linear behavior and the high sensitivity of XA at low concentrations.

The analytical results from the linear part of the calibration curve in Fig. 3 (insert) are summarized in Table 2. The large sensitivity enhancement (sens.$_{expt}$/sens.$_{calc}$) that is observed at low concentrations is in part due to the roughness of the surface of the RPG electrode and the resulting enhanced area for surface interactions (the roughness factor of 6.5 has been reported for RPG [27]), where the active area of the electrode is larger than the geometric electrode area. The large active area fraction of an active electrode [28] can contribute to the fast apparent electron transfer kinetics and to the well-defined voltammograms that are observed (Fig. 2).

The additional effect of the high electrode activity, however, are the fluctuations in the current

apparent form the large error bars in Fig. 3. By comparison at mirror-like RPG higher LOD (10 μm) and larger linear dynamic range have been reported [10].

The sensitivity observed for XA by CV can be compared to that observed previously at RPG for UA (4.89 A M cm^{-2}) [29] in the same low concentration range (after normalization for scan rate since the results have been obtained at different scan rates, 50 mV s^{-1} for UA and 100 mV s^{-1} for XA). The sensitivity is significantly higher than that reported for dopamine (3-hydroxytyramine) and dopac (3,4-dihydroxyphenylacetic acid) at the RPG electrode at high concentrations [18].

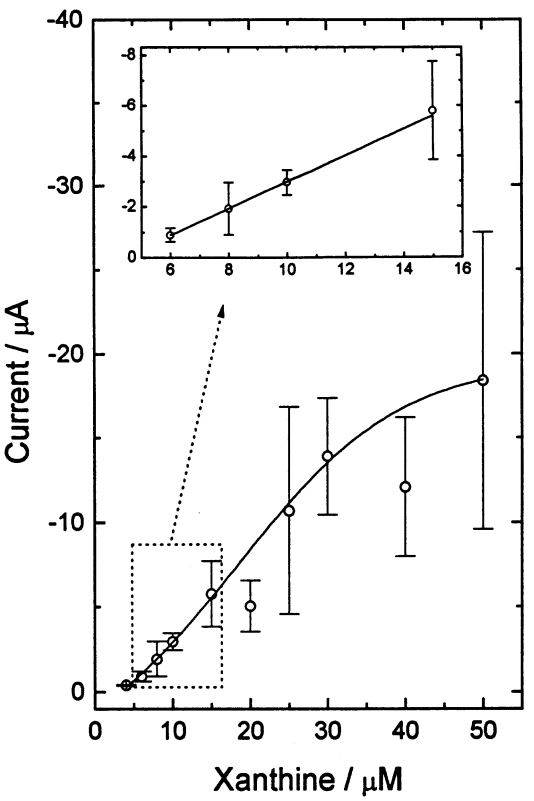

Fig. 3. Cyclic voltammetric current (i_p) versus concentration of XA at the RPG electrode. Experimental conditions as in Fig. 2.

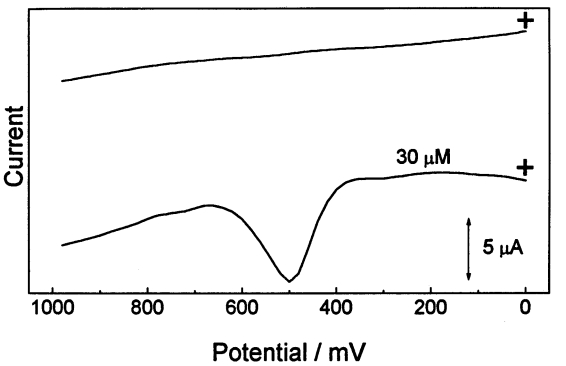

Fig. 4. Differential pulse voltammograms of: XA (bottom curve) and buffer background (top curve) at the RPG electrode ($v = 20$ mV s^{-1}, pulse amplitude 50 mV, sampling time 17 ms, pulse width 50 ms, electrode area 0.04 cm^2). Solution conditions as in Fig. 2.

3.2. Differential pulse voltammetry of XA at the RPG electrodes

DPV can offer an important advantage in the determination of purines because of the capabilities of this technique for efficient separation of the analytical signal from the capacitive background current. This gain can be offset by lower sensitivity, due to preelectrolysis of the analyte, and by the fluctuations of the background current which occur as part of the signal generation/acquisition sequence in DPV. Instability of the electrode surface which is in part determined by the method of electrode treatment [30,31] contributes to the fluctuations of the background current. The fluctuations can be large at active graphite such as RPG as shown by the results of CV. In some cases preelectrolysis can stabilize the background [32].

Because of the differential method of current acquisition in DPV, where the analyte current is obtained as a difference Δi which reaches a maximum at $E_{1/2}$, the sensitivity in DPV is a strong function of electrode kinetics [30]. Of special interest was the effect of the method of the capacitive background subtraction and current acquisition in DPV [30] on the sensitivity of XA.

Fig. 4 illustrates typical DPV results for XA including the background response of the RPG electrode. In DPV, the background current at the RPG electrode is small in phosphate buffer (Fig. 4

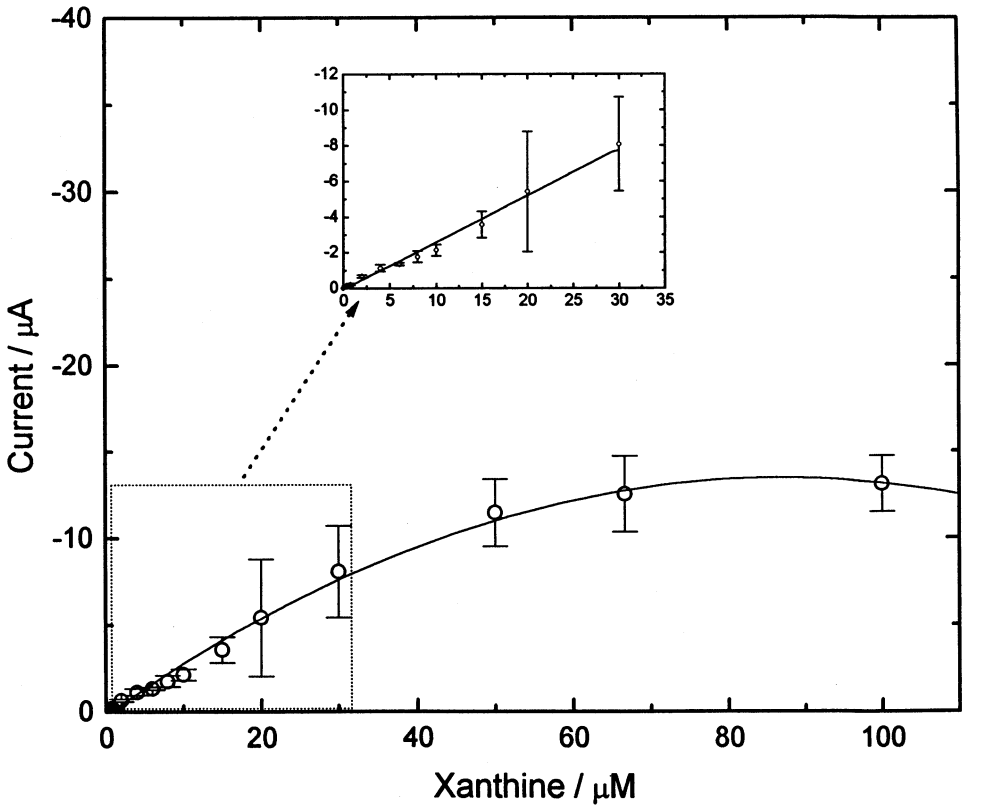

Fig. 5. Differential pulse voltammetric peak current (i_p) versus concentration of XA at the RPG electrode. Conditions as in Fig. 4.

top curve) in the 0.460–0.510 V range where XA responds but, as in CV, this background is not stable. A LOD estimated from the DPV results in Fig. 5 is five times lower than the LOD estimated in CV for XA (Table 2). This verifies that the capacitive background subtraction in DPV in fact improves the LOD even when the background current is not stable as is observed here. The low intercept of the analytical curves (Fig. 5, Table 2) provides direct evidence for efficient background subtraction. The influence of surface processes on the DPV response of XA is confirmed by the non-linear dependence of the current, Δi_{max}, on XA concentration (Fig. 5).

The lower sensitivity of DPV in XA determinations compared to CV (Table 2) is a result of the method of signal acquisition where the maximum signal (Δi_{max}) is measured in the kinetically controlled region (Δi_{max} at $E_{1/2}$) [30]. Furthermore, the sensitivity is lower because of the preelectrolysis of the analyte during the signal acquisition. However, the improved LOD in DPV and the lower capacitive background current are an advantage of the technique. The experimentally observed sensitivity in DPV is higher relative to the theoretical sensitivity estimated for a kinetically slow process [31] (Table 2) and as in CV this enhancement is consistent with a process occurring at an active electrode with an area larger than the geometric electrode area.

3.3. Square wave voltammetry of XA at the RPG electrode

Square wave voltammetry (SWV) offers capabilities for background subtraction (of capacitive and in some cases faradaic background current). In addition, less preelectrolysis in high speed

SWV measurements limits the depletion of analyte. This leads to an increase in sensitivity with an increase in frequency of SWV [30]. However, short pulse duration of each pulse in SWV can result in a kinetically limited electrode process and can enhance the influence of surface processes on the measured signal [30,33].

For processes controlled by slow kinetics, measurement of the forward current produces the most sensitive response [33]. Under the range of the conditions tested (frequency 15–60 Hz) in the determinations of XA the sensitivity is best for the forward current (Fig. 6) in agreement with the behavior for a kinetically slow process.

The LOD of XA in SWV is the lowest of the methods tested (Table 2) and current above background can be detected for 50 nM XA presumably as a result of efficient background subtraction; from the results, the LOD of XA is estimated to be 200 nM.

In the linear dynamic range the sensitivity to XA is higher in SWV than in DPV; the sensitivity enhancement is similar in SWV and DPV (Table 2). Rapid signal acquisition with less preelectrolysis and efficient capacitive background subtraction are responsible for the high sensitivity [30]; the added advantage is the electrode with a large active area.

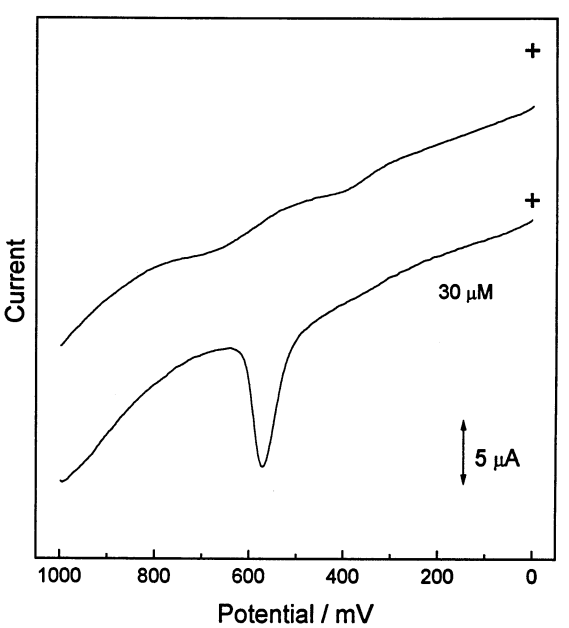

Fig. 6. Forward square wave voltammogram of: XA (bottom curve) and buffer background (top curve) at the RPG electrode (frequency 60 Hz, step height 2 mV, $v = 120$ mV s^{-1}, electrode area 0.04 cm^2). Solution conditions as in Fig. 2.

Fig. 7 shows the non-linear dependence of SWV current on XA concentration which is consistent with the control of XA response by surface processes, in agreement with the results of CV and DPV. The larger fluctuations of the current in SWV evident from the large error bars reflect higher sensitivity of SWV and greater instability of the electrode in fast SWV measurements compared to DPV.

3.4. Cyclic voltammetry of XA at carbon fiber ultramicroelectrodes

The radius of the carbon fiber UME determined by CV in ferricyanide solutions for a disk electrode is in a reasonable agreement with the radius reported by the manufacturer, $r = 2.85 \pm 0.01$ and 7 μm diameter, respectively.

Because of the practical limitations in resurfacing of the carbon fiber UME the electrodes were reused and their stability was tested with use. The electrodes initially polished on 600-grit silicon carbide paper and with γ-alumina showed reasonable stability after a series of XA determinations by CV in phosphate buffer. This is in agreement with lower sensitivity and relatively low activity of the polished electrodes (Table 2). The 75 mV slope of the log $i_p - i/i$ versus E plot confirms low surface activity of the polished carbon fiber UME and apparent slow electron transfer kinetics of XA (Fig. 8b). Apparent kinetics of ferricyanide were also slow at these electrodes as indicated by the 70 ± 6 mV slope of the log $i_l - i/i$ versus E plot.

The stability of the surface of the 600-grit/alumina polished carbon fiber UME in CV was further verified by measuring XA current before and after obtaining a calibration curve. For 8 μM XA the current was 1.60 ± 0.25 and $1.57 \pm 0.46 \times 10^{-2}$ nA, respectively, confirming the stability of the surface. Similarly, after many determinations of the same concentration of XA (20 μM, 5 measurements and 67 μM, 5 and 20 measurements) a stable current was observed. However,

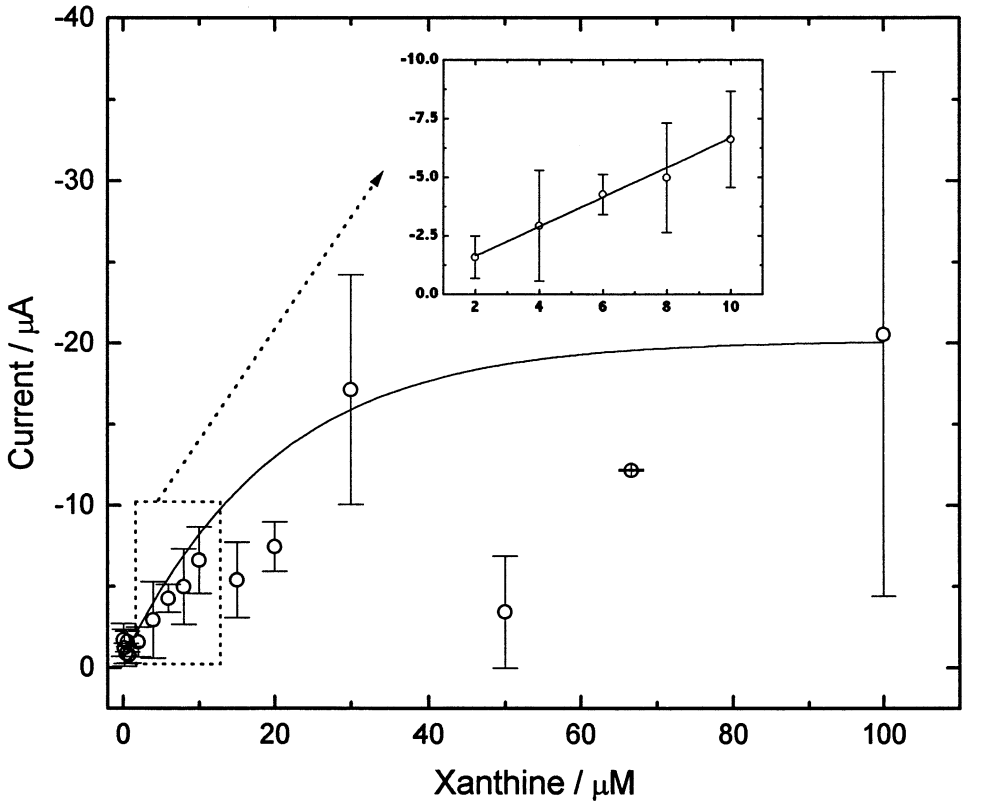

Fig. 7. Forward square wave voltammetric peak current (i_p) versus concentration of XA at the RPG electrode. Experimental conditions as in Fig. 6.

carbon fiber UMEs polished on 150-grit silicon carbide paper, and then on 600-grit paper and with γ-alumina, showed a significant decrease in surface activity with use. This was shown by a decrease in ferricyanide current (63% decrease in the apparent electrode radius was determined) whereas electrodes polished on 600-grit paper and γ-alumina showed a more stable response (29% change in the apparent radius) after use.

The mass transport to an UME, at slow CV scan rates, is very efficient [34,35] and can enhance the effect of surface processes on the current; surface processes will control the overall process if they are slow relative to the mass and electron transport [36]. Fig. 9 compares the analytical curves that were obtained at UMEs at different carbon fiber surfaces: the electrochemically pretreated (Fig. 9a), new 600-grit polished (Fig. 9b) and 150-grit polished (Fig. 9c). Control of the XA current by surface processes is apparent from the shape of the analytical curves which show the same non-linear behavior with concentration, with saturation at higher XA concentrations, that was observed at the RPG electrodes. High sensitivity is observed at active carbon fiber surfaces produced by electrochemical pretreatment and by polishing on 150-grit paper (Table 2, Fig. 9).

As shown by the results which are summarized in Table 2 the sensitivity of carbon fiber UMEs in XA determinations is a function of the electrode treatment. The sensitivity of the active electrodes (such as the electrochemically pretreated electrode; Fig. 9, Table 2) is significantly higher and is very high compared to the sensitivity of 0.04 cm^2 area RPG electrodes. This is in part due to a small background at an UME ($i_{bkg} \sim$ area $\sim r^2$) relative to the analytical signal ($i \sim r$) [34,35] and

to the method of signal measurement in the mass transport controlled region. Nevertheless, the high sensitivity does not result in a significant improvement in LOD because of the inefficient method of background subtraction in CV.

3.5. Cyclic voltammetry of HX

The electrochemical oxidation of HX is an overall 4e, $4H^+$ process and involves the formation of 6,8-dioxypurine as an intermediate [24]. The intermediate is formed in a 2e, $2H^+$ oxidation which proceeds with an addition of an oxygen to the C8 of the purine ring. The electrochemical oxidation of HX occurs at more positive potentials than the oxidation of XA (HX

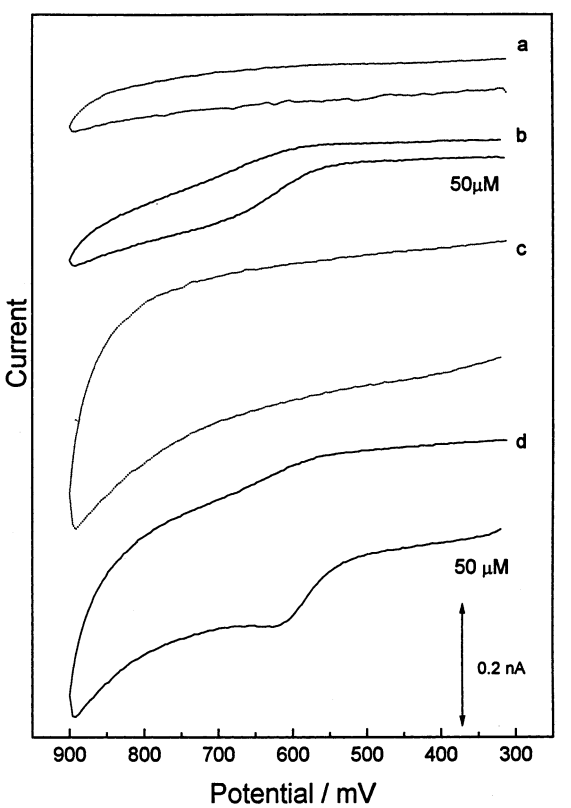

Fig. 8. Cyclic voltammograms of 50 μM XA (b,d) and the buffer background (a,c) at 600-grit/alumina polished (a,b) and electrochemically pretreated carbon fiber ultramicroelectrode (c,d). Scan rate $v = 100$ mV s^{-1} electrode radius 2.8×10^{-4} cm. Experimental conditions as in Fig. 6.

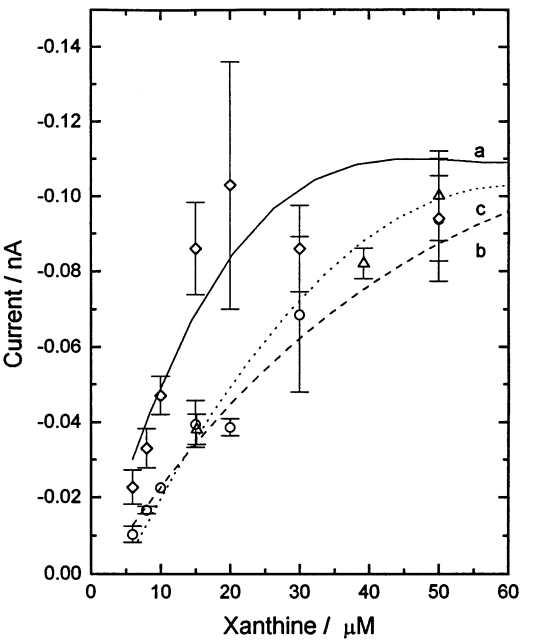

Fig. 9. Ultramicroelectrode current versus concentration of XA at: (a) electrochemically pretreated carbon fiber (–◇–); (b) new 600-grit/alumina polished (--○--); (c) 150-grit polished (···△···) carbon fiber.

contains one less oxygen) and, in spite of the same number of electrons and protons in the overall oxidation of XA and HX and the same initial step in the oxidation which involves an addition of an oxygen to C8, the final oxidation products of XA and HX are different and the oxidations involve different pathways [22,24].

Cyclic voltammetry of HX at the RPG electrode shows a single oxidation peak between 0.880 and 0.895 V (Fig. 10). The non-linear dependence of the peak current i_p on concentration shows the contribution of surface processes to the oxidation as observed for XA. Fig. 11 shows the dependence of the current (i_p) on the concentration of HX in CV at the RPG electrode. The analytical figures of merit summarized in Table 2 show that the sensitivity in CV is lower for HX than for XA. This may indicate that surface interactions apparent form the non-linear dependence of the current on the concentration (Fig. 11) contribute less to HX than to XA oxidation current; current- concentration plot shows saturation at higher concentrations of HX than of XA.

The LOD obtained for HX by CV is 4 μM as for XA (Table 2) indicating that the sensitivity to HX and XA is limited in CV by the capacitive background current. Based on these results it is possible to conclude that the analytical response of both purines is determined by the activity of the electrode and the method of signal acquisition. At the RPG electrodes, the results for HX follow the results for XA, with lower sensitivity observed for HX.

4. Conclusions

The purpose of this work was to determine the sensitivity and the LOD that can be achieved under physiologically relevant conditions in the electrochemical determinations of XA and HX. Although only synthetic samples were used in these determinations it has been previously shown that phosphate buffer at physiological pH is a relevant model medium for bioanalysis [37].

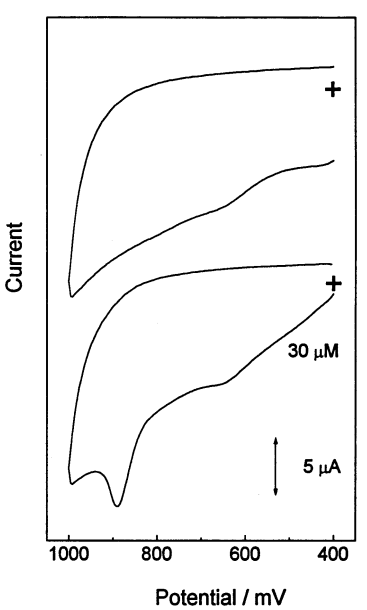

Fig. 10. Cyclic voltammograms of HX at the RPG electrode. Experimental conditions as in Fig. 1.

Different methods of activation of pyrolytic graphite and carbon fiber electrodes were compared and different methods of signal acquisition were evaluated at these electrodes for their sensitivity in the determinations of XA and HX. The results show that high sensitivity can be achieved in the determinations of both oxypurines at the electrodes that were produced. The high sensitivity can be achieved with fast methods of signal acquisition such as SWV which is important in view of the complex multielectron oxidations of oxypurines. Such oxidations can be slow and, thus, can lead to low sensitivity.

In addition, as expected, there is evidence from the results that the active large area electrodes facilitate the interactions of oxypurines with the electrode surface, and the interactions appear to play an important role in the high sensitivity of the determinations. Finally the results provide some evidence for a slow kinetic step, that may be related to a surface process, in the oxidations of the oxypurines at the active electrodes.

Based on previous predictions [30], amperometric methods which efficiently separate the capacitive background current from the measured signal show the lowest LOD in the determinations of oxypurines, although this does not always translate into the best sensitivity for the methods, presumably because the methods can, for example, additionally lead to fluctuations in the electrode background current. One reason for the fluctuations may be oxidation of the graphite surface and associated changes of the electrode area.

The results also show that at carbon fiber UMEs with a large active electrode area high sensitivity is observed, the highest measured by any methods.

The results shown here demonstrate the feasibility of the development of new electroanalytical methods for the determination of oxypurines in biological samples. The results illustrate the influence of different parameters such as electrode activity and stability, and speed of measurements on the sensitivity of the determinations. The results show that such parameters have to be optimized independently for best performance in these determinations.

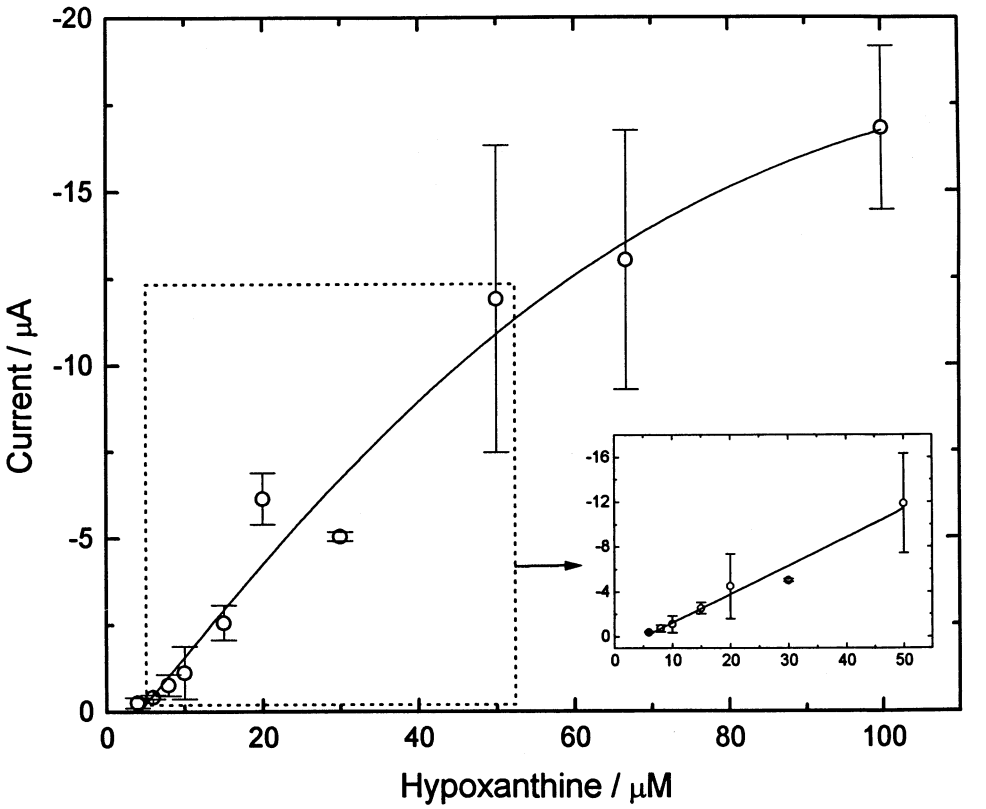

Fig. 11. Cyclic voltammetric current (i_p) versus concentration of HX at the RPG electrode. Conditions as in Fig. 10.

Acknowledgements

ETGC acknowledges the support through a fellowship from Fundação de Amparo à Pesquisa do Estado de São Paulo (FAPESP/ Brazil) and Universidade Federal de São Carlos, São Carlos/ SP/Brazil.

References

[1] W.T. Caraway, Stand. Methods Clin. Chem. 4 (1963) 239–247.
[2] R.A. Harkness, J. Chromatogr. Biomed. Appl. 429 (1988) 255–278.
[3] D. Crushing, S. Mustafa, Adenosine and Adenosine Nucleotides as Regulators of Cellular Functions, CRC Press, Boca Raton, FL, 1991.
[4] S. Glodowski, R. Bilewicz, Z. Kublik, Anal. Chim. Acta 186 (1986) 39–47.
[5] B.C. Household, C.M.G. Van den Berg, J.P. Riley, Anal. Chim. Acta 200 (1987) 291–303.
[6] R.M. Shubietah, A.Z. Abu-Zuhri, A.G. Fogg, Electroanalysis 7 (1995) 975–979.
[7] M.S. Ibrahim, M.E. Ahmed, Y.M. Temerk, A.M. Kawde, Anal. Chim. Acta 328 (1996) 47–52.
[8] M.S. Ibrahim, M.E. Ahmed, A.M. Kawde, Y.M. Temerk, Analusis 24 (1996) 6–9.
[9] E. Palacek, Anal. Biochem. 108 (1980) 129–138.
[10] R.N. Goyal, A. Mittal, S. Sharma, Electroanalysis 6 (1994) 609–611.
[11] J.L. Owens, G. Dryhurst, Anal. Chim. Acta 89 (1977) 93–99.
[12] R.M. Ianniello, T.J. Lindsay, A.M. Yacynych, Anal. Chem. 54 (1982) 1980–1984.
[13] K. McKenna, A. Brajter-Toth, Anal. Chem. 59 (1987) 954–958.
[14] G. Arai, S. Takahashi, I. Iasumori, J. Electroanal. Chem. 410 (1996) 173–179.
[15] H.G. Xue, S.L. Mu, J. Electroanal. Chem. 397 (1995) 241–247.
[16] T. Yao, Anal. Chim. Acta 281 (1993) 323–326.
[17] C.C. Hsueh, R. Bravo, A. Jaramillo, A. Brajter-Toth, Anal. Chim. Acta 349 (1997) 67–76.

[18] A. Marino, A. Brajter-Toth, Anal. Chem. 65 (1993) 370–374.
[19] M. Stackelberg, M. Pilgram, V. Toome, Z. Elektrochem. 57 (1953) 342–350.
[20] C.C. Hsueh, A. Brajter-Toth, Anal. Chim. Acta 321 (1996) 209–214.
[21] C.C. Hsueh, R. Bravo, A. Jaramillo, A. Brajter-Toth, Analyst (in press).
[22] B.H. Hansen, G. Dryhurst, J. Electroanal. Chem. 30 (1971) 417–426.
[23] A. Albert, D.J. Brown, J. Chem. Soc., (1954) 2060–2073.
[24] A.C. Conway, R.N. Goyal, G. Dryhurst, J. Electroanal. Chem. 123 (1981) 243–264.
[25] A.J. Bard, L.R. Faulkner, Electrochemical Methods, Wiley, New York, 1980.
[26] A. Marino, A. Brajter-Toth, Chem. Anal. (Warsaw) 40 (1995) 565–578.
[27] L. Bodalbhai, A. Brajter-Toth, Anal. Chim. Acta 231 (1990) 191–201.
[28] (a) C. Amatore, J.M. Saveant, D. Tessier, J. Electroal. Chem. 147 (1983) 39–51. (b) M.S. Freund, A. Brajter-Toth, J. Electroanal. Chem. 300 (1991) 347–363.
[29] R. Bravo, University of Florida, unpublished results.
[30] J.G. Osteryoung, Acc. Chem. Res. 26 (1993) 77–83.
[31] J.G. Osteryoung, R.A. Osteryoung, Anal. Chem. 57 (1985) 101A–110.
[32] M. Regino, A. Brajter-Toth, Anal. Chim. Acta 369 (1998) 253–262.
[33] M.J. Nuwer, J.J. O'Dea, J.G. Osteryoung, Anal. Chim. Acta 251 (1991) 13–25.
[34] Y. Saito, Rev. Polarogr. Jpn. 15 (1968) 177–187.
[35] J. Heinze, Angew. Chem. Int. Ed. Eng. 32 (1993) 1268–1288.
[36] Q. Cheng, A. Brajter-Toth, Anal. Chem. 68 (1996) 4180–4185.
[37] N.E. Good, S. Izawa, in: A. San Pietro (Ed.), Methods in Enzymology 24 (Part B), Academic Press, New York, 1972, pp. 53–68.